AGU PUBLICATIONS

Paleoceanography

RESEARCH ARTICLE
10.1002/2017PA003149

Sensitivity of the Greenland Ice Sheet to Interglacial Climate Forcing: MIS 5e Versus MIS 11

Rima Rachmayani[1,2], Matthias Prange[1,3], Daniel J. Lunt[4], Emma J. Stone[4], and Michael Schulz[1,3]

[1]Faculty of Geosciences, University of Bremen, Bremen, Germany, [2]Department of Oceanography, Faculty of Earth Science and Technology, Bandung Institute of Technology, Bandung, Indonesia, [3]MARUM-Center for Marine Environmental Sciences, University of Bremen, Bremen, Germany, [4]BRIDGE, School of Geographical Sciences, University of Bristol, Bristol, UK

Key Points:
- Output from CCSM3 interglacial climate simulations used to force ice sheet model
- Stronger sensitivity of the Greenland ice sheet to MIS 11 climate forcing than to MIS 5 forcing
- Strong Atlantic overturning contributes to MIS 11 Greenland ice sheet melt

Correspondence to:
R. Rachmayani,
rrachmayani@oceanography.itb.ac.id

Citation:
Rachmayani, R., Prange, M., Lunt, D. J., Stone, E. J., & Schulz, M. (2017). Sensitivity of the Greenland Ice Sheet to interglacial climate forcing: MIS 5e versus MIS 11. *Paleoceanography*, *32*, 1089–1101. https://doi.org/10.1002/2017PA003149

Received 16 MAY 2017
Accepted 5 SEP 2017
Accepted article online 23 SEP 2017
Published online 3 NOV 2017

Abstract The Greenland Ice Sheet (GrIS) is thought to have contributed substantially to high global sea levels during the interglacials of Marine Isotope Stage (MIS) 5e and 11. Geological evidence suggests that the mass loss of the GrIS was greater during the peak interglacial of MIS 11 than MIS 5e, despite a weaker boreal summer insolation. We address this conundrum by using the three-dimensional thermomechanical ice sheet model Glimmer forced by Community Climate System Model version 3 output for MIS 5e and MIS 11 interglacial time slices. Our results suggest a stronger sensitivity of the GrIS to MIS 11 climate forcing than to MIS 5e forcing. Besides stronger greenhouse gas radiative forcing, the greater MIS 11 GrIS mass loss relative to MIS 5e is attributed to a larger oceanic heat transport toward high latitudes by a stronger Atlantic meridional overturning circulation. The vigorous MIS 11 ocean overturning, in turn, is related to a stronger wind-driven salt transport from low to high latitudes promoting North Atlantic Deep Water formation. The orbital insolation forcing, which causes the ocean current anomalies, is discussed.

1. Introduction

Continental ice sheets are a major factor in the climate change debate, in particular due to their direct link to global sea level. The study of warm climates in the past may provide useful insight into the sensitivity of polar land ice to changing forcing. A growing body of evidence suggests particularly high global sea levels along with significant shrinking of the Greenland Ice Sheet (GrIS) during the Quaternary interglacials of Marine Isotope Stage (MIS) 5e and MIS 11 (Colville et al., 2011; Dutton et al., 2015; Hatfield et al., 2016; Reyes et al., 2014; Schaefer et al., 2016; Strunk et al., 2017).

For the interglacial of MIS 5e, the Last Interglacial (LIG; ~130–115 kyr ago), global mean annual temperature was estimated to have been 0.5–1°C warmer than during the preindustrial (Dutton et al., 2015; Hoffman et al., 2017; Otto-Bliesner et al., 2013), while summer temperature anomalies might have been up to 5°C above present in the Arctic region reflecting substantial polar amplification (e.g., Last Interglacial Project Members, 2006; NEEM community members, 2013; Otto-Bliesner et al., 2006). Compilations of relative sea level combined with modeling suggest a LIG peak global mean sea level of 6–9 m above present (Dutton & Lambeck, 2012; Dutton et al., 2015; Kopp et al., 2009, 2013; O'Leary et al., 2013). The contribution of GrIS melting to this sea level rise is highly uncertain, but model results suggest a GrIS contribution between 1.4 and 4.3 m (Born & Nisancioglu, 2012; Helsen et al., 2013; Masson-Delmotte et al., 2013; Quiquet et al., 2013; Robinson et al., 2011; Stone et al., 2013), indicating that the size of the GrIS was still substantial during the LIG (Colville et al., 2011; Yau et al., 2016). It has been demonstrated, however, that the simulation of LIG GrIS mass loss is highly sensitive to poorly constrained model parameters (Stone et al., 2013).

Meanwhile, a warm interglacial during MIS 11 ~ 420–395 kyr ago (Dutton et al., 2015; Milker et al., 2013) has been suggested a potential analogue for present and future climate (Alley et al., 2010; Bowen, 2010; Droxler et al., 2003; Loutre and Berger, 2000, 2003) when orbital geometry was similar to the configuration during the present interglacial (Berger & Loutre, 1991). A peak of global mean temperature anomaly of up to 2°C might have existed during MIS 11 relative to preindustrial although there is high uncertainty in the global average temperature at that time (Dutton et al., 2015; Lang & Wolff, 2011; Masson-Delmotte et al., 2010). Evidence from marine sediment cores points to sea surface temperatures (SST) in the North Atlantic 1–2°C higher than today

(Bauch et al., 2000; De Abreu et al., 2005; Helmke et al., 2003; Kandiano & Bauch, 2003; McManus et al., 1999). Furthermore, a minimum GrIS extent during the MIS 11 interglacial implies a likely loss of most of the Greenland ice mass (Hatfield et al., 2016; Reyes et al., 2014), contributing to a maximum global mean sea level during the MIS 11 interglacial likely 6–13 m higher than today (Chen et al., 2014; Dutton et al., 2015; Muhs et al., 2012; Raymo & Mitrovica, 2012; Roberts et al., 2012).

Taken together, mass loss of the GrIS was likely greater during the interglacial of MIS 11 than during the LIG. Since the changing seasonal insolation owing to varying astronomical parameters is thought to be a major forcing of polar ice sheet evolution (e.g., Huybers, 2006; Loutre et al., 2004; van de Berg et al., 2011), the great GrIS mass loss during MIS 11 seems to be counterintuitive. Due to a low eccentricity of the Earth's orbit, climatic precession varied relatively little during MIS 11, and hence, maximum boreal summer insolation was much smaller during the MIS 11 interglacial than during the LIG (Figure 1). By contrast, eccentricity was high during the LIG leading to high summer insolation values around 125 ka. Huybers (2006) pointed out that glaciers are sensitive to insolation integrated over the duration of the summer and introduced the concept of the integrated summer insolation as the dominant control on polar ice sheet evolution. Like maximum summer insolation, values for the integrated summer insolation were larger during the LIG than during MIS 11 (Figure 1) and cannot simply explain a stronger GrIS melting during MIS 11 compared to MIS 5e. Moreover, the concept of accumulated insolation (Carlson & Winsor, 2012), which incorporates intensity and duration of orbital forcing, also fails to explain the interglacial extent of the GrIS over the past 430,000 years, in particular the lack of appreciable southern GrIS retreat during MIS 7 (Hatfield et al., 2016). On the other hand, greenhouse gas (GHG) concentrations were higher during MIS 11 compared to the LIG and the duration was longer (Figure 1).

Using the three-dimensional thermomechanical ice sheet model Glimmer (Genie land ice model with multiply-enabled regions), the sensitivity of GrIS mass loss to interglacial climate forcing of MIS 5e and 11 is studied in the present work. Climate forcing comes from MIS 5e and MIS 11 simulations with the Community Climate System Model version 3 (CCSM3). We will address the conundrum as to why the GrIS mass loss may have been greater during MIS 11 than during MIS 5e despite a weaker summer insolation. Note that we do not examine the role of interglacial duration in driving MIS 11 deglaciation, as it has recently been done by Robinson et al. (2017).

2. Experimental Setup

2.1. Models

2.1.1. CCSM3 Global Climate Model

The coupled general circulation model (CGCM) CCSM3 is composed of four components representing atmosphere, ocean, sea ice, and land surface (Collins et al., 2006). We used the low-resolution (T31) version of the model (Yeager et al., 2006). In this version, the horizontal resolution of the atmosphere and land components is 3.75° with 26 layers in the atmosphere, while the nominal resolution of the ocean/sea ice grid is 3°. The ocean grid consists of 25 levels in the vertical. In this study, the dynamic global vegetation model is included along with some improvements of land hydrology parameterizations (Oleson et al., 2008) as in previous studies (e.g., Handiani et al., 2013; Rachmayani et al., 2015, 2016).

2.1.2. Glimmer Ice Sheet Model

To simulate the GrIS response to interglacial climate forcing provided by CCSM3, we use the three-dimensional thermomechanical ice sheet model Glimmer version 1.0.4 (Payne, 1999; Rutt et al., 2009). The model is constructed on a Cartesian grid with horizontal resolution of 20 km along with 11 layers in the vertical. A shallow ice approximation is used for the ice dynamics. At each time step, surface air temperature and surface mass balance are taken as input fields. The time step for the ice dynamics is 1 year. The surface mass balance is simulated using the positive degree day (PDD) approach as explained in Reeh (1991), DeConto and Pollard (2003), and Lunt et al. (2008, 2009). The PDD method is based on the assumption that the surface ice melt is proportional to the time-integrated temperature above freezing point which provides for the energy available for melting. To consider different albedos and densities, different PDD factors are applied for ice and snow (Stone et al., 2013). Glimmer further assumes an elastic isostatic response of the lithosphere to changes in ice mass. Bilinear interpolation is utilized to map the forcing data taken from the low-resolution CCSM3 climate model onto the high-resolution Glimmer grid. Moreover, a lapse rate correction is applied in converting the surface air temperature from CCSM3 to the ice model grid which represents the local aspect of the temperature elevation feedback. Further details on the ice sheet model and its offline coupling to the atmosphere can be found in Lunt et al. (2008) and Stone et al. (2013, 2010).

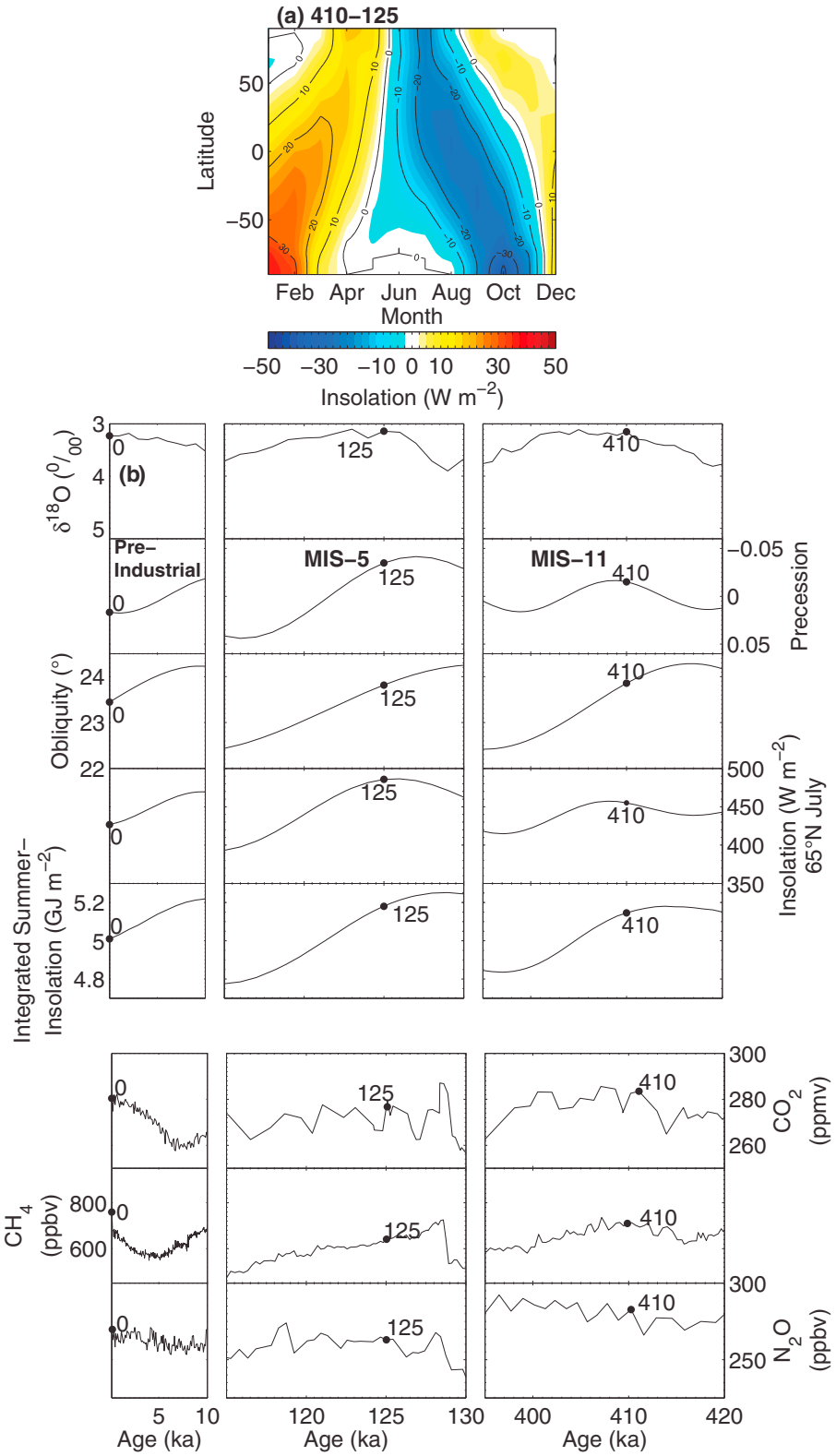

Figure 1. (a) Insolation anomalies between 410 and 125 ka. The calculation assumes a fixed present-day calendar with vernal equinox at 21 March. (b) Benthic $\delta^{18}O$ stack (Lisiecki & Raymo, 2005), climatic precession, obliquity, July insolation at 65°N (Berger, 1978), the integrated summer insolation with $\tau = 275$ W/m^2 according to Huybers (2006), and GHG concentrations (Loulergue et al., 2008; Lüthi et al., 2008; Schilt et al., 2010) for the Holocene, MIS 5e, and MIS 11. GHG concentrations for the industrial era are not shown. The dots mark the time slices simulated in this study.

Table 1
GHG Concentrations Used in the CCSM3 Experiments

Experiments	CO_2 (ppmv)	CH_4 (ppbv)	N_2O (ppbv)
0 ka (PI)	280	760	270
125 ka (MIS 5e)	276	640	263
410 ka (MIS 11)	284	710	282

2.2. Setup of Experiments

2.2.1. Climate Experiments

Climate forcing for the ice sheet model is provided by two CCSM3 interglacial time slice experiments, one with 125 ka boundary conditions (MIS 5e) and the other with 410 ka boundary conditions (MIS 11). Table 1 provides the boundary conditions which include astronomical parameters (Berger, 1978) and atmospheric GHG concentrations. The ice sheet configuration, ozone distribution, sulfate aerosols, carbonaceous aerosols, and solar constant were maintained identical to the preindustrial (PI) control run. GHG concentrations for the MIS 5e time slice were taken as specified by the Paleoclimate Modelling Intercomparison Project (PMIP3; Lunt et al., 2013) and GHG concentrations for the MIS 11 time slice are based on Loulergue et al. (2008), Lüthi et al. (2008), and Schilt et al. (2010) using the European Project for Ice Coring in Antarctica Dome C time scale EDC3 (Figure 1). Both interglacial time slice simulations were branched off from year 600 of the PI spin-up run and integrated for 400 years each, which was sufficient for the surface climate and the Atlantic meridional overturning circulation (AMOC; Figure 2) to come to a statistical equilibrium. A standard PI control run was integrated for 1,000 years, and it was performed following PMIP guidelines (Braconnot et al., 2007). For details on the CCSM3 PI and interglacial time slice experiments the reader is referred to Kleinen et al. (2014), Lunt et al. (2013), and Rachmayani et al. (2016). Precipitation and near-surface air temperature from the last 100 years of each experiment were taken to force the Glimmer ice sheet model.

2.2.2. Ice Sheet Experiments

The ice sheet model was spun-up for 50,000 years using modern climatological ERA-40 data sets (Hanna et al., 2005, 2008; ECMWF, 2006) and the Greenland bedrock topography of Bamber et al. (2001). Subsequently, the forcing was switched to interglacial climate of the 125 ka and 410 ka time slices, respectively, using simulated precipitation and temperature anomalies (relative to the control run) added to the ERA-40 climatology Stone et al. (2013, 2010).

For each time slice experiment, six Glimmer simulations with different sets of tuning parameters were performed. This has been done to test the robustness of our Glimmer results with respect to some poorly constrained parameters that influence ice dynamics and surface mass balance in large-scale ice sheet modeling. The six parameter sets (Table 2) were identified by Stone et al. (2010) as optimal in Glimmer simulations of the GrIS, yielding the best fits to observed present-day GrIS geometry according to different diagnostics (ice surface extent, total ice volume, maximum ice thickness, and spatial fit of ice thickness) and skill scores. The six optimal parameter sets were identified among 250 plausible parameter sets using a latin hypercube sampling, which is an efficient variant of the Monte Carlo approach. Experiments nos. 10 and 233 by Stone et al. (2010) yielded the best fit for ice volume and ice thickness distribution, experiment 99 yielded the best fit for ice surface extent, experiment 165 was optimal with respect to ice surface extent and ice thickness distribution, and experiments 67 and 240 simulated maximum ice thickness most accurately. The different parameter sets include five tuneable parameters, that is, the flow enhancement factor, geothermal heat flux, lapse rate, and the two PDD factors. Lapse rate and PDD factors are fundamental in controlling surface ablation.

The goal of our model experiments is not to simulate a realistic evolution of the GrIS during the interglacials of MIS 5e and MIS 11, as this would require a transient climate forcing as well as feedbacks from the ice sheet

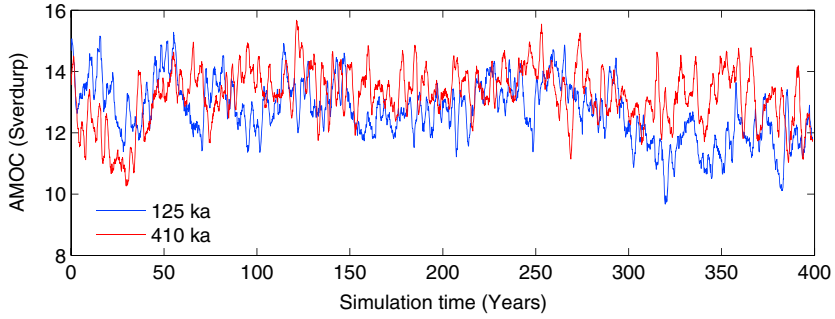

Figure 2. Time series of the AMOC stream function at 28°N and 1,000 m depth smoothed with a 24 month filter for the 410 ka (red) and 125 ka (blue) experiments, in sverdrups. After spin-up the 410 ka AMOC is systematically stronger than the 125 ka AMOC.

Table 2
Tuned Parameter Values Used in the Glimmer Ice Sheet Experiments

Experiment no.	f	L_G (°C km^{-1})	G (mW m^{-2})	α_s (mm d^{-1} °C^{-1})	α_i (mm d^{-1} °C^{-1})
10	4.5838	−4.2047	−52.630	3.7243	19.878
233	4.8585	−4.0754	−46.667	4.2425	16.344
99	1.2838	−4.5334	−41.758	4.7844	18.710
165	3.1036	−4.2456	−47.709	4.5763	19.455
67	2.6165	−8.1157	−53.421	3.9951	13.502
240	2.5551	−6.0820	−59.070	3.6258	10.221

Note. The tuning parameters are f (flow enhancement factor), L_G (near-surface lapse rate), G (geothermal heat flux), α_s (PDD factor for snow), and α_i (PDD factor for ice). The experiment numbers (tuning parameter settings) are taken from Stone et al. (2010) and have been identified as optimal with respect to the simulation of the modern GrIS. For details the reader is referred to Stone et al. (2010).

to the climate model components. Instead, our goal is to identify potential mechanisms in the climate system that may have been responsible for the strong GrIS mass loss during MIS 11 compared to the LIG. Since we consider the 125 ka and 410 ka time slices representative of the LIG and the peak interglacial of MIS 11 in terms of insolation and GHG forcing (Figure 1), we deem our time slice approach appropriate for this purpose.

3. Results

3.1. Ice Sheets Simulated by Glimmer

A rapid decline of the GrIS volume takes place within a few thousand years after switching the climate forcing from modern to either 125 ka (Figure 3a) or 410 ka (Figure 3b). For both time slices it is evident that the simulated size of the GrIS strongly depends on the set of tuning parameters used. For both interglacials, experiment 67 reveals the highest sensitivity to the 125 ka and 410 ka forcings such that the GrIS almost disappears in less than 5,000 years. Experiment 67 is characterized by the largest lapse rate L_G (Table 2), which probably leads to an overestimation of the positive temperature elevation feedback.

However, independent of the tuning parameter set used, the GrIS mass loss is always greater in the MIS 11 experiments compared to the MIS 5e experiments. Surface ablation is the dominant factor for the greater

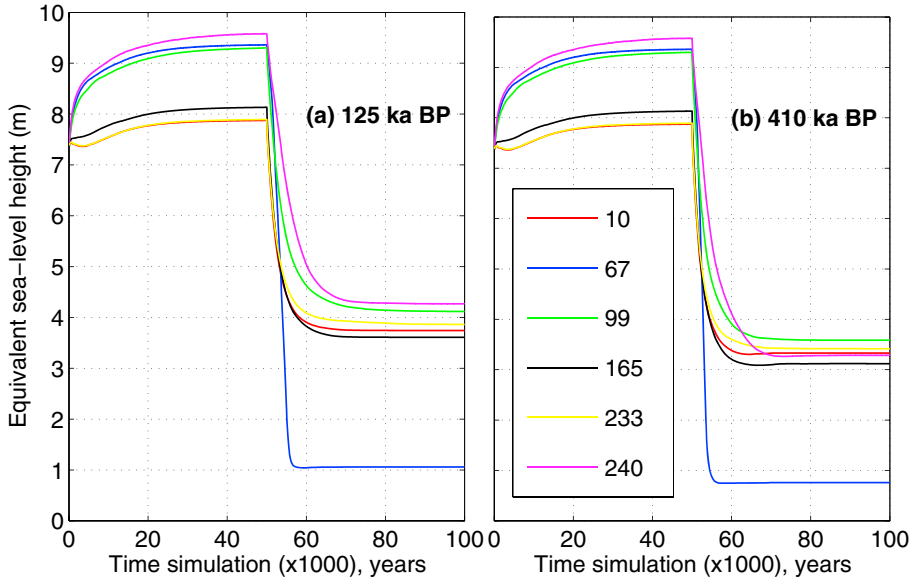

Figure 3. Results from the Glimmer MIS 5e and MIS 11 experiments: Time series of GrIS volume as equivalent sea level height for (a) the 125 ka and (b) the 410 ka experiment (switching from modern to interglacial climate forcing at model year 50,000) using different tuning parameter settings (see Table 2).

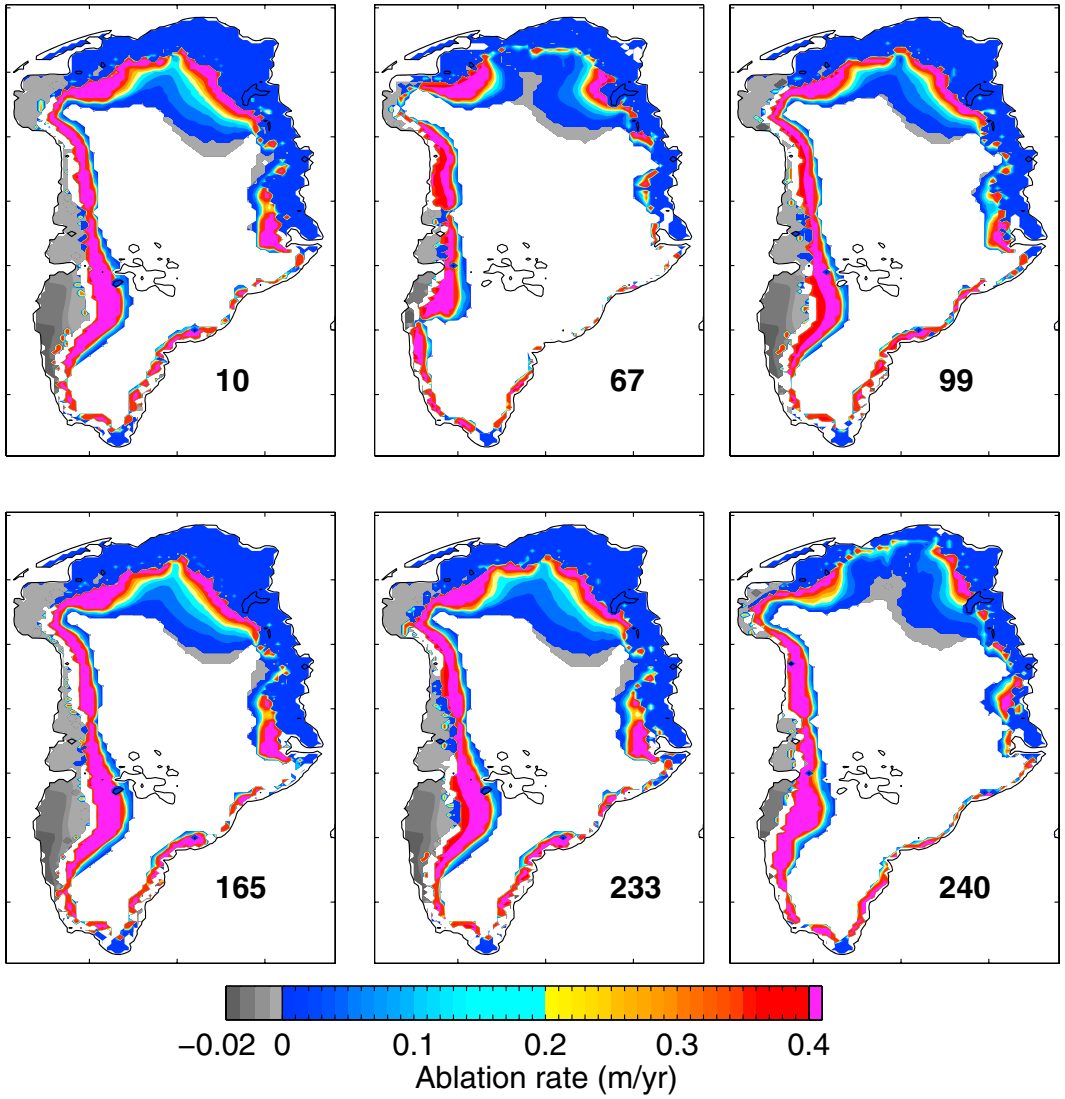

Figure 4. Ablation rate anomalies (410 ka minus 125 ka experiment) at model year 500 after switching from modern to interglacial climate forcing for different tuning parameter settings (see Table 2).

MIS 11 ice loss. Figure 4 shows higher ablation rates in the MIS 11 experiments compared to the LIG, especially in northern, northeastern, and western Greenland, independent of the tuning parameter settings. Given the weaker summer insolation forcing during MIS 11 compared to the LIG (Figure 1), the generally higher ablation rates seem counterintuitive.

3.2. Climatic Fields Simulated by CCSM3

Figure 5 shows the difference between the climate forcings of MIS 11 (410 ka) and MIS 5e (125 ka) as provided by CCSM3. Higher MIS 11 summer (June-July-August, JJA) air temperatures across Greenland compared to the LIG provide the energy required for the enhanced surface melting (Figure 5a), while the annual deposition of snow due to precipitation is greater in MIS 11 than in MIS 5e over most parts of Greenland except for the southernmost and southwestern portion (Figure 5b). This precipitation anomaly pattern is associated with southeasterly wind anomalies over the eastern Greenland region favoring the supply of moisture from the North Atlantic and Nordic Seas and northerly wind anomalies over western Greenland favoring the transport of dry Arctic air toward the south (Figure 6a). Therefore, enhanced snowfall tends to counteract the larger MIS 11 GrIS mass loss associated with surface ablation over large regions. Higher GHG concentrations (Table 1) contribute to the anomalously warm conditions in Greenland during MIS 11 (Yin & Berger, 2015).

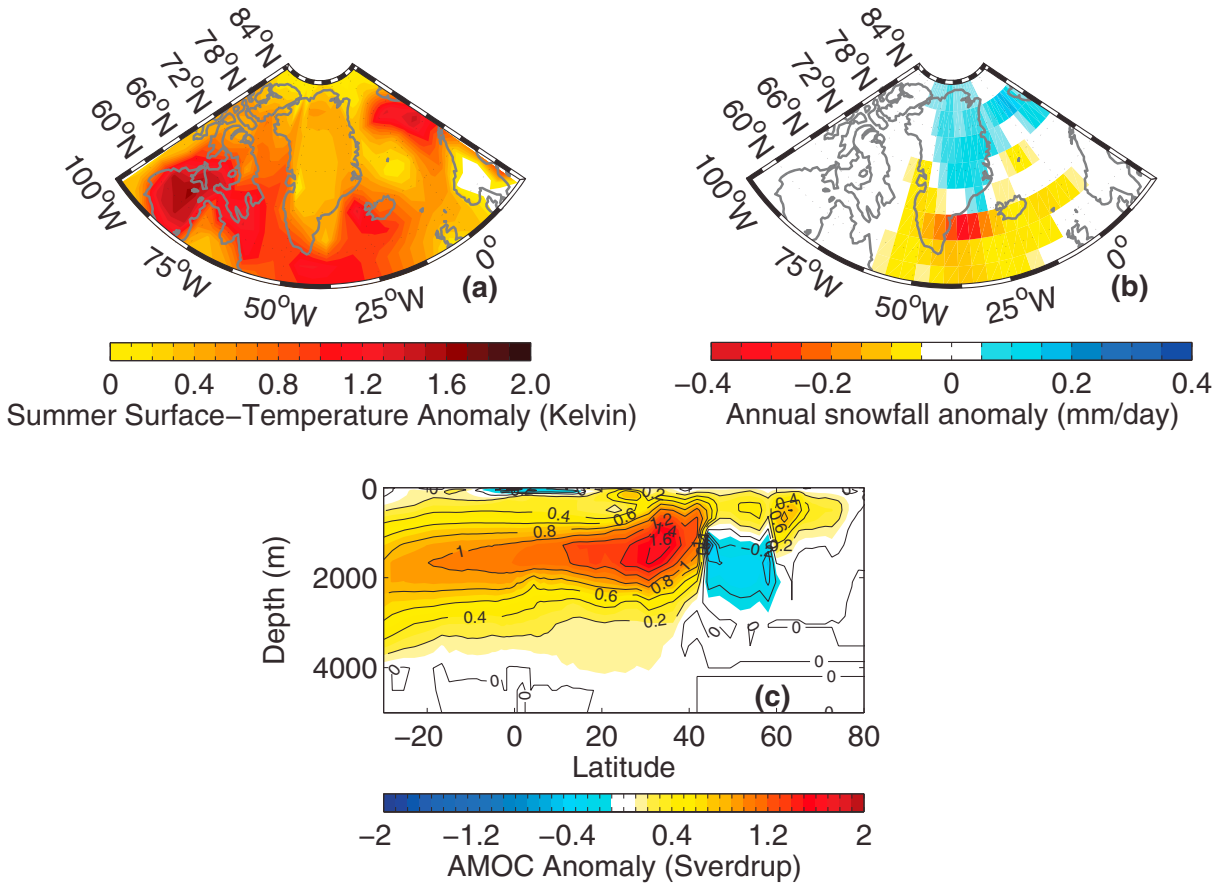

Figure 5. Differences between 410 ka (MIS 11) and 125 ka (MIS 5e) of climatic fields simulated by CCSM3: (a) boreal summer (JJA) surface temperature in and around Greenland, (b) annual snowfall, and AMOC (meridional overturning stream function in the Atlantic Ocean).

However, a closer inspection of the summer surface temperature anomaly pattern reveals a maximum in the North Atlantic and Nordic Seas pointing to changes in the large-scale ocean circulation (Figure 5a). A comparison of the ocean circulations between the different experiments shows that the AMOC is about 1.7 sverdrup (Sv) (1 Sv = 10^6 m^3/s) stronger in the MIS 11 time slice compared to the LIG experiment (Figures 2 and 5c), thus transporting more heat (~ 8–15% increase depending on latitude) from the tropical North Atlantic to subpolar regions, where air-sea heat exchange takes place with impact on the climate over Greenland. Compared to the modern control run, the AMOC at 125 ka is even 2.2 Sv weaker.

4. AMOC Strengthening During MIS 11

A major, albeit not the only, factor controlling North Atlantic Deep Water formation, and hence the AMOC, is salinity due to its effect on seawater density. A higher sea surface salinity in most regions of the extratropical North Atlantic in the MIS 11 experiment compared to the LIG experiment is therefore consistent with enhanced deep water formation (Figure 6c). The higher sea surface salinity in the northern North Atlantic can be caused by a reduced surface freshwater flux forcing (associated with a change in the hydrologic cycle) and/or by increased advection of salt from lower latitudes (due to a change in ocean currents). Figure 6d shows the difference in surface freshwater flux forcing between the MIS 11 and LIG experiments. The net freshwater flux into the northern North Atlantic is larger in the MIS 11 experiment than in the LIG and hence cannot explain the higher MIS 11 surface salinity. Instead, the barotropic stream function indicates an anomalously strong transport of (high saline and warm) subtropical water from Florida Strait toward the northeastern North Atlantic (Figure 6b), involving a stronger Gulf Stream in the MIS 11 simulation. A larger salt transport creates more saline conditions in the northern North Atlantic favoring deep water formation and a stronger AMOC. The horizontal ocean circulation anomaly, in turn, is to first-order attributable to differences in the wind

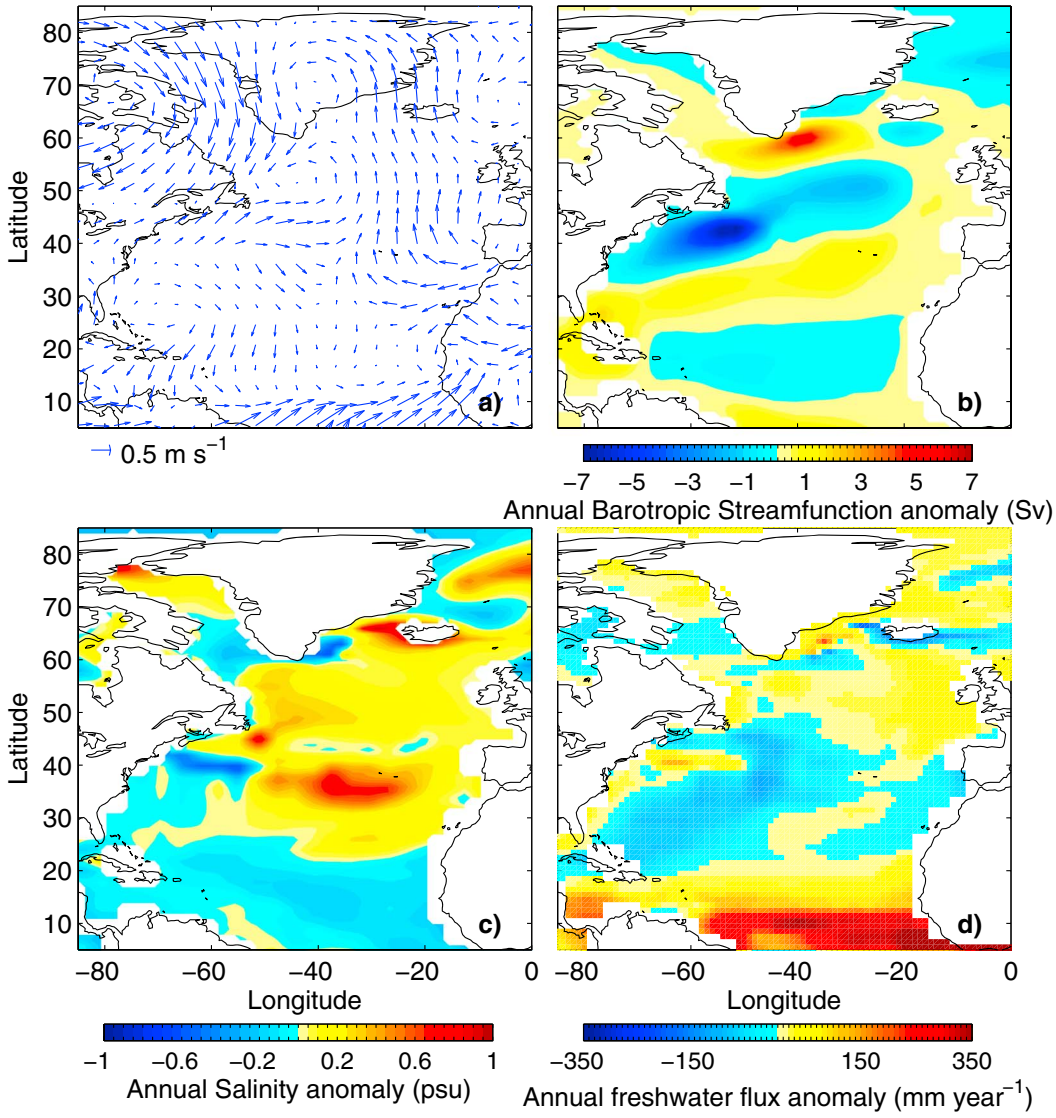

Figure 6. Annual differences between 410 ka (MIS 11) and 125 ka (MIS 5e) of climatic and oceanic fields simulated by CCSM3 in the North Atlantic: (a) surface wind, (b) barotropic stream function (positive in clockwise direction), (c) sea surface salinity, and (d) surface freshwater flux (positive into the ocean).

stress forcing owing to the Sverdrup relation, which states that the meridional mass transport is balanced by the curl of the wind stress (e.g., Gill, 1982). Figure 6a shows the annual-mean surface wind difference between the MIS 11 and LIG experiments. In the northeastern Atlantic (north of ~45°N) the wind anomaly field is cyclonic (i.e., positive wind stress curl anomaly) leading to an anomalous northward Sverdrup transport, which is associated with an anomalous cyclonic gyre centered at 50°N shown in the barotropic stream function plot (Figure 6b). Between ~25 and 40°N the surface wind anomaly field over the eastern North Atlantic is anticyclonic (Figure 6a). The negative wind stress curl anomaly results in an anomalous southward Sverdrup transport associated with an anomalous anticyclonic gyre (Figure 6b), which—together with the anomalous cyclonic gyre to the north—conveys more high-saline subtropical water toward high latitudes in the MIS 11 experiment promoting deep water formation there. The important role of wind-driven salt advection toward high latitudes in driving the AMOC has been demonstrated in previous model studies (Oka et al., 2001; Timmermann & Goosse, 2004). A stronger AMOC, in turn, may further support the northward transport of salt from the subtropics to higher latitudes, thus creating a positive feedback (Stommel, 1961).

While the major differences in ocean circulation and salinity fields between the MIS 11 and LIG experiments can be understood by means of different wind forcing, the differences in the annual-mean wind fields

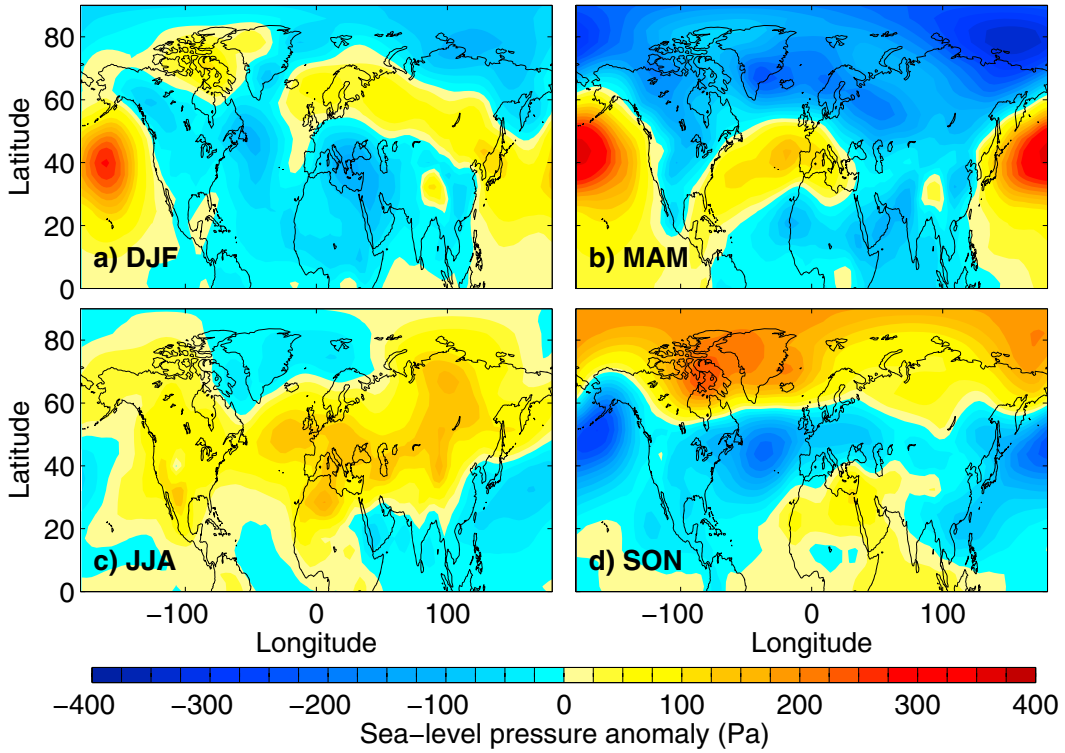

Figure 7. Seasonal SLP anomalies between 410 ka (MIS 11) and 125 ka (MIS 5e) during Northern Hemisphere (a) winter (DJF), (b) spring (MAM), (c) summer (JJA), and (d) autumn (SON).

(Figure 6a), in turn, are more challenging to interpret. However, some important insight into atmospheric dynamics of the MIS 11 and LIG experiments and their relation to insolation forcing can be obtained by analyzing seasonal differences, from which the annual-mean wind field anomaly derives. Figure 7 shows differences in sea level pressure (SLP) for each season. In boreal summer (June–August), a weaker insolation at 410 ka compared to 125 ka (Figure 1a) leads to less heating and hence higher SLP over the continents (Figure 7c). In boreal winter (December–February) and spring (March–May), the situation is almost opposite with predominantly lower SLP over continental regions in the MIS 11 experiment (Figures 7a and 7b) due to higher insolation compared to the MIS 5e experiment (Figure 1a). An interesting situation arises in boreal autumn (September–November), when a reduced late summer/early autumn Northern Hemisphere meridional insolation gradient in the MIS 11 experiment compared to the MIS 5e experiment gives rise to anomalously high/low SLP in high/middle latitudes (Figure 7d), involving slower winds at the northern flank of the westerlies. This season dominates the annual-mean surface wind anomaly between MIS 11 and the LIG over the mid-latitude North Atlantic, with its cyclonic structure north of ~ 45°N (Figure 6a) and hence is crucial for the ocean current anomalies that drive the enhanced northward salt transport and stronger AMOC in the MIS 11 experiment.

5. Response of the GrIS to Interglacial Climate Forcings

Equal or even greater GrIS mass loss during the interglacial of MIS 11 compared to the LIG is difficult to explain with pure insolation forcing. In harmony with geological evidence our model experiments suggest stronger GrIS melt during the interglacial of MIS 11 than during the LIG. The northern and western regions of Greenland show the strongest sensitivities to MIS 11 interglacial climate forcing.

The stronger MIS 11 ice loss relative to the LIG is attributable to higher Greenland summer surface temperatures. Given the higher summer insolation in the MIS 5e experiment compared to the MIS 11 experiment (Figure 1a), other processes must be responsible for the warm MIS 11 summer temperatures. Indeed, the boreal summer season shows a much smaller MIS 11 Greenland surface temperature anomaly (relative to the LIG) than the other seasons, consistent with the insolation forcing (taking approximately 1 month time lag between insolation forcing and regional temperature response into account). However, there is an

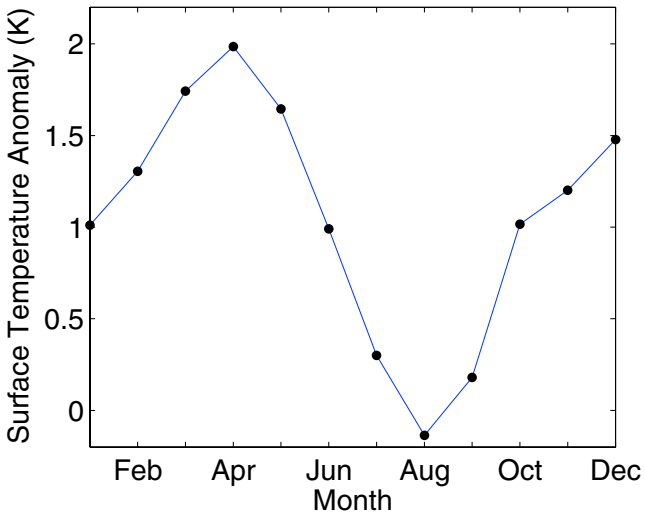

Figure 8. Difference in monthly mean Greenland (66–82°N, 50–30°W) surface temperature between 410 ka (MIS 11) and 125 ka (MIS 5e), annual cycle.

annual-mean Greenland temperature offset of 1.0°C in MIS 11 relative to the LIG, which eventually gives rise to the warmer MIS 11 summer temperatures responsible for enhanced GrIS melt (Figure 8). We identify three mechanisms that lead to almost year-round warm anomalies in the Greenland/North Atlantic region in the MIS 11 experiment compared to the LIG: (i) a stronger AMOC which transports more heat to high northern latitudes, (ii) enhanced greenhouse gas concentrations which corresponds to a radiative forcing of 0.25 W m^{-2}, and (iii) a slightly larger obliquity (Figure 1b) which results in a larger annual-mean insolation forcing of about 0.4 W m^{-2} at 70°N. Through changes in surface albedo, a smaller Arctic sea ice area during the MIS 11 interglacial (not shown) may act as a positive feedback to the anomalous warming in high latitudes.

Our results suggest that the maximum summer insolation forcing is much less important for the GrIS surface melting and evolution of mass balance during interglacials than often assumed. It has been shown previously that seasonal temperature variations to orbital insolation forcing are significantly smaller in Greenland than in other continental regions (Rachmayani et al., 2016), which may be attributable to the higher albedo and proximity to the ocean which strongly damps seasonal variability.

Warm Greenland summer conditions during the LIG in response to high insolation have been simulated by numerous climate models (e.g., Kaspar et al., 2005; Lunt et al., 2013; Montoya et al., 2000; Otto-Bliesner et al., 2006; Stone et al., 2013). Unfortunately, only few model studies exist regarding the climate of MIS 11. Simulations with the Earth system model of intermediate complexity LOVECLIM show colder Greenland summer temperatures during the MIS 11 peak interglacial compared to the LIG (Yin & Berger, 2012, 2015), in contrast to our results. In the absence of proxy records from Greenland which date back to MIS 11 it is not possible to assess which model result is more realistic. Paleoceanographic studies from the northern North Atlantic are inconclusive as to whether summer SSTs where warmer or colder during the MIS 11 peak interglacial compared to the LIG, as the results depend on the paleothermometric method used (Kandiano & Bauch, 2003). However, some evidence exists for strong North Atlantic Deep Water formation and a vigorous Atlantic overturning during the MIS 11 interglacial (Vazquez Riveiros et al., 2013).

Our approach does not allow a quantitative estimate of LIG and MIS 11 GrIS volumes due to several limitations of the experimental setup. First, the climatic forcing of the ice sheet model is stationary (time slice approach) rather than transient as in, for example, Stone et al. (2013). Moreover, the modeled ice sheet does not feed back to the other climate components (offline coupling), like the atmosphere and the ocean. In particular, GrIS meltwater flux into the ocean might further affect the AMOC and hence North Atlantic and Greenland temperatures (Yang et al., 2016). Future studies should therefore simulate the MIS 5e and MIS 11 GrIS evolution in interactively coupled CGCM-ice sheet transient experiments. Ideally, such transient experiments would include the preceding terminations and glacials as these may precondition the evolution of the subsequent interglacials (cf. Dendy et al., 2017; Past Interglacials Working Group of PAGES, 2016). Second, the semiempirical PDD scheme used in calculating the surface mass balance may significantly underestimate surface melt associated with high insolation. van de Berg et al. (2011) have shown that a direct effect of stronger summer insolation and also the related nonlinear feedbacks drive enhanced surface melting along with the higher ambient temperature. As a result, taking insolation and albedo explicitly into account would likely lead to a greater GrIS mass loss under high insolation forcing, especially during the LIG. Third, as shown by Stone et al. (2013) and in the present study, the simulation of GrIS volumes strongly depends on different tuning parameters. Even though a set of tuning parameters yields a realistic simulation of the modern GrIS (as do all parameter sets used in this study; see Table 2), this does not ensure a realistic simulation of the LIG or MIS 11 ice sheet using the same set of parameters. An insightful example was given by experiment 67, in which the GrIS almost completely disappeared within a few thousand years in response to both LIG and MIS 11 climate forcing. A too high value for the lapse rate was identified to be the main cause for this outcome. We further note that the near-surface lapse rate over Greenland may be climate dependent (Erokhina et al., 2017).

Further caveats, mostly related to simplifications of the ice sheet dynamics, are discussed in Stone et al. (2010) and Stone et al. (2013). These shortcomings aside, our model results suggest hitherto overlooked processes to explain strong MIS 11 GrIS melt, such as a wind-driven amplification of the AMOC and associated heat transport. A recent model study by Robinson et al. (2017) has emphasized the role of MIS 11's long duration as an important factor for the GrIS to disappear almost completely (see also Reyes et al., 2014), while Hatfield et al. (2016) highlighted the role of CO_2. We would like to point out that the different proposed factors for the strong MIS 11 Greenland deglaciation do not rule out each other but may well have acted together.

6. Conclusions

MIS 5e and MIS 11 interglacial experiments with the Glimmer ice sheet model driven by CCSM3 climate model output suggest a stronger sensitivity of the GrIS to MIS 11 climate forcing than to MIS 5e forcing. We attribute the greater MIS 11 ice loss relative to the LIG in large part to a greater heat transport toward high northern latitudes by a stronger AMOC. The MIS 11 AMOC is amplified by anomalous wind stress curl that drives enhanced salt transport from the low- to high-latitude North Atlantic. A reduced Northern Hemisphere meridional insolation gradient in late summer/early autumn in MIS 11 compared to the LIG sets the appropriate wind forcing that drives the ocean current anomaly. Our model results demonstrate that Quaternary GrIS volume changes are not a simple function of orbital insolation. Instead, internal climate feedbacks have to be considered when interpreting the long-term waxing and waning of the GrIS. Further studies of MIS 11 climate with other general circulation models need to be performed in order to assess the robustness of the CCSM3 results.

Acknowledgments
This study was supported by the Deutsche Forschungsgemeinschaft (DFG) through the priority research program INTERDYNAMIC (SPP 1266). The CCSM3 model simulations have been carried out using the supercomputer of the Norddeutscher Verbund fuer Hoch- und Hoechstleistungsrechnen (HLRN). The Glimmer model simulations have been conducted at the School of Geographical Sciences, University of Bristol, during a research stay of R. R. The model results presented in this manuscript are available in PANGAEA database (https://doi.pangaea.de/10.1594/PANGAEA.879318). We thank the PAGES Working Groups on Past Interglacials (PIGS) and Quaternary Interglacials (QUIGS) for discussions and support. We are grateful to the anonymous reviewers and A. E. Carlson for their helpful suggestions and constructive comments which substantially improved the paper.

References

Alley, R. B., Andrews, J. T., Brigham-Grette, J., Clarke, G. K. C., Cuffey, K. M., Fitzpatrickf, J. J., … White, J. W. C. (2010). History of the Greenland Ice sheet: Paleoclimate insights. *Quaternary Science Reviews*, *29*, 1728–1756. https://doi.org/10.1016/j.quascirev.2010.02.007

Bamber, J. L., Layberry, R., & Gogineni, P. (2001). A new ice thickness and bed data set for the Greenland ice sheet 1. Measurement, data reduction, and errors. *Journal Geophysical Research*, *106*, 33,773–33,780. https://doi.org/10.1029/2001JD900054

Bauch, H. A., Erlenkeuser, H., Helmke, J. P., & Struck, U. (2000). A paleoclimatic evaluation of marine oxygen isotope stage 11 in the high-northern Atlantic (Nordic seas). *Global and Planetary Change*, *24*, 2–39.

Berger, A. (1978). Long-term variations of daily insolation and Quaternary climatic changes. *Journal of the Atmospheric Sciences*, *35*, 2362–2367.

Berger, A., & Loutre, M. F. (1991). Insolation values for the climate of the last 10 million years. *Quaternary Science Reviews*, *10*, 297–317. https://doi.org/10.1016/0277-3791(91)90033-Q

Born, A., & Nisancioglu, K. H. (2012). Melting of Northern Greenland during the last interglaciation. *The Cryosphere*, *6*, 1239–1250. https://doi.org/10.5194/tc-6-1239-2012

Bowen, D. Q. (2010). Sea level 400,000 years ago (MIS 11): Analogue for present and future sea-level? *Climate of the Past*, *6*, 19–29.

Braconnot, P., Otto-Bliesner, B., Harrison, S., Joussaume, S., Peterchmitt, J.-Y., Abe-Ouchi, A., … Zhao, Y. (2007). Results of PMIP2 coupled simulations of the mid-Holocene and Last Glacial Maximum — Part 1: Experiments and large-scale features. *Climate of the Past*, *3*, 261–277. https://doi.org/10.5194/cp-3-261-2007

Carlson, A. E., & Winsor, K. (2012). Northern Hemisphere ice-sheet responses to past climate warming. *Nature Geoscience*, *5*, 607–613.

Chen, F., Friedman, S., Gertler, C. G., Looney, J., O'Connell, N., Sierks, K., & Mitrovica, J. X. (2014). Refining estimates of polar ice volumes during the MIS 11 Interglacial using sea level records from South Africa. *Journal of Climate*, *27*, 8740–8746. https://doi.org/10.1175/JCLI-D-14-00282.1

Collins, W. D., Bitz, C. M., Blackmon, M. L., Bonan, G. B., Bretherton, C. S., Carton, J. A., … Smith, R. D. (2006). The Community Climate System Model version 3 (CCSM3). *Journal of Climate*, *19*, 2122–2143. https://doi.org/10.1175/JCLI3761.1

Colville, E. J., Carlson, A. E., Beard, B. L., Hatfield, R. G., Stoner, J. S., Reyes, A. V., & Ullman, D. J. (2011). SrNdPb isotope evidence for ice-sheet presence on southern Greenland during the last interglacial. *Science*, *333*, 620–623. https://doi.org/10.1126/science.1204673

De Abreu, C., Abrantes, F. F., Shackleton, N. J., Tzedakis, P. C., McManus, J. F., Oppo, D. W., & Hall, M. A. (2005). Ocean climate variability in the eastern North Atlantic during interglacial marine isotope stage 11 e a partial analogue to the Holocene? *Paleoceanography*, *20*, PA3009. https://doi.org/10.1029/2004PA001091

DeConto, R. M., & Pollard, D. (2003). Rapid Cenozoic glaciation of Antarctica induced by declining atmospheric CO_2. *Nature*, *421*, 245–249. https://doi.org/10.1038/nature01290

Dendy, S., Austermann, J., Creveling, J., & Mitrovica, J. X. (2017). Sensitivity of Last Interglacial sea-level high stands to ice sheet configuration during Marine Isotope Stage 6. *Quaternary Science Reviews*, *171*, 234–244. https://doi.org/10.1016/j.quascirev.2017.06.013

Droxler, A. W., Alley, R. B., Howard, W. R., Poore, R. Z., & Burckle, L. H. (2003). Unique and exceptionally long interglacial marine isotope stage 11 window into Earth future climate. In A. W. Droxler, R. Z. Poore & L. H. Burckle (Eds.), *Earth's Climate and Orbital Eccentricity: The Marine Isotope Stage 11 Question, Geophysical Monograph* (pp. 1–14), Washington, DC: American Geophysical Union. https://doi.org/10.1029/137GM01

Dutton, A., Carlson, A. E., Long, A. J., Milne, G. A., Clark, P. U., DeConto, R., … Raymo, M. E. (2015). Sea-level rise due to polar ice-sheet mass loss during past warm periods. *Science*, *349*, 6244. https://doi.org/10.1126/science.aaa4019

Dutton, A., & Lambeck, K. (2012). Ice volume and sea level during the last interglacial. *Science*, *337*, 216–219. https://doi.org/10.1126/science.1205749

ECMWF (2006). *ECMWF ERA-40 re-analysis data*. Retrieved from British Atmospheric Data Centre: http://badc.nerc.ac.uk/browse/badc/ecmwf-e40/data

Erokhina, O., Rogozhina, I., Prange, M., Bakker, P., Bernales, J., Paul, A., & Schulz, M. (2017). Dependence of slope lapse rate over the Greenland ice sheet on background climate. *Journal of Glaciology*, *63*(239), 568–572. https://doi.org/https://doi.org/10.1017/jog.2017.10

Gill, A. E. (1982). *Atmosphere-Ocean Dynamics* (662 pp.). San Diego: Academic Press.

Hanna, E., Huybrechts, P., Janssens, I., Cappelen, J., Steffen, K., & Stephens, A. (2005). Runoff and mass balance of the Greenland ice sheet: 1958–2003. *Journal Geophysical Research*, *110*, D13108. https://doi.org/10.1029/2004JD005641

Hanna, E., Huybrechts, P., Steffen, K., Cappelen, J., Huff, R., Shuman, C., … Grifths, M. (2008). Increased runoff from melt from the Greenland Ice Sheet: A response to global warming. *Journal of Climate*, *21*, 331–341. https://doi.org/10.1175/2007JCLI1964.1

Handiani, D., Paul, A., Prange, M., Merkel, U., Dupont, L., & Zhang, X. (2013). Tropical vegetation response to Heinrich Event 1 as simulated with the UVic ESCM and CCSM3. *Climate of the Past*, *9*, 1683–1696. https://doi.org/10.5194/cp-9-1683-2013

Hatfield, R. G., Reyes, A. V., Stoner, J. S., Carlson, A. E., Bard, B. L., Winsor, K., & Welke, B. (2016). Interglacial responses of the Southern Greenland ice sheet over the last 430,000 years determined using particle-size specific magnetic and isotopic tracers. *Earth and Planetary Science Letters*, *454*, 225–236. https://doi.org/10.1016/j.epsl.2016.09.014

Helmke, J. P., Bauch, H. A., & Erlenkeuser, H. (2003). Development of glacial and interglacial conditions in the Nordic seas between 1.5 and 0.35 Ma. *Quaternary Science Reviews*, *22*, 1717–1728. https://doi.org/10.1016/S0277-3791(03)00126-4

Helsen, M. M., van de Berg, W. J., van de Wal, R. S. W., van den Broeke, M. R., & Oerlemans, J. (2013). Coupled regional climate-ice-sheet simulation shows limited Greenland ice loss during the Eemian. *Climate of the Past*, *9*, 1773–1788. https://doi.org/10.5194/cp-9-1773-2013

Hoffman, J. S., Clark, P. U., Parnell, A. C., & He, F. (2017). Regional and global sea-surface temperatures during the last interglaciation. *Science*, *355*(6322), 276–279. https://doi.org/10.1126/science.aai8464

Huybers, P. (2006). Early Pleistocene glacial cycles and the integrated summer insolation forcing. *Science*, *313*, 508–511. https://doi.org/10.1126/science.1125249

Kandiano, E. S., & Bauch, H. A. (2003). Surface ocean temperatures in the north-east Atlantic during the last 500,000 years: Evidence from foraminiferal census data. *Terra Nova*, *15*, 265–271. https://doi.org/10.1046/j.1365-3121.2003.00488X

Kaspar, F., Kuhl, N., Cubasch, U., & Litt, T. (2005). A model-data comparison of European temperatures in the Eemian interglacial. *Geophysical Research Letter*, *32*, L11703. https://doi.org/10.1029/2005GL022456

Kleinen, T., Hildebrandt, S., Prange, M., Rachmayani, R., Müller, S., Bezrukova, S., … Tarasov, P. (2014). The climate and vegetation of Marine Isotope Stage 11—Model results and proxy-based reconstructions at global and regional scale. *Quaternary International*, *348*, 247–265. https://doi.org/10.1016/j.quaint.2013.12.028

Kopp, R. E., Simons, F. J., Mitrovica, J. X., Maloof, A. C., & Oppenheimer, M. (2009). Probabilistic assessment of sea level during the last interglacial stage. *Nature*, *462*, 863–868. https://doi.org/10.1038/nature08686

Kopp, R. E., Simons, F. J., Mitrovica, J. X., Maloof, A. C., & Oppenheimer, M. (2013). A probabilistic assessment of sea level variations within the last interglacial stage. *Geophysical Journal International*, *193*, 711–716. https://doi.org/10.1093/gji/ggt029

Lang, N., & Wolff, E. W. (2011). Interglacial and glacial variability from the last 800 ka in marine,ice and terrestrial archives. *Climate of the Past*, *7*, 361–380. https://doi.org/10.5194/cp-7-361-2011

Last Interglacial Project Members, CAPE (2006). Last Interglacial Arctic warmth confirms polar amplification of climate change. *Quaternary Science Reviews*, *25*, 1383–1400. https://doi.org/10.1016/j.quascirev.2006.01.033

Loulergue, L., Schilt, A., Spahni, R., Masson-Delmotte, V., Blunier, T., Lemieux, B., … Chappellaz, J. (2008). Orbital and millennial-scale features of atmospheric CH_4 over the past 800,000 years. *Nature*, *453*, 383–386.

Loutre, M. F., & Berger, A. (2000). Future climatic changes: Are we entering an exceptionally long interglacial? *Climatic Change*, *46*, 61–90. https://doi.org/10.1023/A:1005559827189

Loutre, M. F., & Berger, A. (2003). Marine isotope stage 11 as an analogue for the present interglacial. *Global and Planetary Change*, *36*(3), 209–217. https://doi.org/10.1016/S0921-8181(02)00186-8

Loutre, M. F., Paillard, D., Vimeux, F., & Cortijo, E. (2004). Does mean annual insolation have the potential to change the climate?. *Earth and Planetary Science Letters*, *221*, 1–14. https://doi.org/10.1016/S0012-821X(04)00108-6

Lisiecki, L. E., & Raymo, M. E. (2005). A Pliocene-Pleistone stack of 57 globally distributed benthic $\delta^{18}O$ records. *Paleoceanography*, *20*, PA1003. https://doi.org/10.1029/2004PA001071

Lunt, D. J., Abe-Ouchi, A., Bakker, P., Berger, A., Braconnot, P., Charbit, S., … Zhang, Z. S. (2013). A multi-model assessment of last interglacial temperatures. *Climate of the Past*, *9*, 699–717. https://doi.org/10.5194/cp-9-699-2013

Lunt, D. J., Foster, G. L., Haywood, A. M., & Stone, E. J. (2008). Late Pliocene Greenland glaciation controlled by a decline in atmospheric CO_2 levels. *Nature*, *454*, 1102–1105. https://doi.org/10.1038/nature07223

Lunt, D. J., Haywood, A. M., Foster, G. L., & Stone, E. J. (2009). The Arctic cryosphere in the Mid-Pliocene and the future. *Philosophical Transactions of the Royal Society of London, Series A: Mathematical, Physical and Engineering Sciences*, *367*, 49–67. https://doi.org/10.1098/rsta.2008.0218

Lüthi, D., Le Floch, M., Bereiter, B., Blunier, T., Barnola, J.-M., Siegenthaler, U., … Stocker, T. F. (2008). High-resolution carbon dioxide concentration record 650,000–800,000 years before present. *Nature*, *453*, 379–382.

Masson-Delmotte, V., Schulz, M., Abe-Ouchi, A., Beer, J., Ganopolski, A., Gonzalez Rouco, J. F., … Timmermann, A. (2013). Information from paleoclimate archives. In T. F. Stocker, D. Qin, G. K. Plattner, M. Tignor, S. K. Allen, J. Boschung, … P. M. Midgley (Eds.), *Climate Change 2013: The Physical Science Basis. Contribution of Working Group I to the Fifth Assessment Report of the Intergovernmental Panel on Climate Change*. Cambridge, United Kingdom and New York: Cambridge University Press.

Masson-Delmotte, V., Stenni, B., Pol, K., Braconnot, P., Cattani, O., Falourd, S., & Kageyama, M. (2010). EPICA Dome C record of glacial and interglacial intensities. *Quaternary Science Reviews*, *29*, 113–128. https://doi.org/10.1016/j.quascirev.2009.09.030

McManus, J. F., Oppo, D. W., & Cullen, J. L. (1999). A 0.5-million year record of millennial-scale climate variability in the North Atlantic. *Science*, *283*, 971–975. https://doi.org/10.1126/science.283.5404.971

Milker, Y., Rachmayani, R., Weinkauf, M. F. G., Prange, M., Raitzsch, M., Schulz, M., & Kučera, M. (2013). Global and regional sea surface temperature trends during marine isotope stage 11. *Climate of the Past*, *9*, 2231–2252. https://doi.org/10.5194/cp-9-2231-2013

Montoya, M., von Storch, H., & Crowley, T. J. (2000). Climate simulation for 125 kyr BP with a coupled ocean-atmosphere general circulation model. *Journal of Climate*, *13*, 1057–1072.

Muhs, D. R., Pandolfi, J. M., Simmons, K. R., & Schumann, R. R. (2012). Sea-level history of past interglacial periods from uranium-series dating of corals, Curaao, Leeward Antilles islands. *Quaternary Research*, *78*, 157–169. https://doi.org/10.1016/j.yqres.2012.05.008

NEEM community members (2013). Eemian interglacial reconstructed from a Greenland folded ice core. *Nature*, *493*, 489–494. https://doi.org/10.1038/nature11789

Oka, A., Hasumi, H., & Suginohara, N. (2001). Stabilization of thermohaline circulation by wind-driven and vertical diffusive salt transport. *Climate Dynamics*, *18*, 71–83.

O'Leary, M. J., Hearty, P. J., Thompson, W. G., Raymo, M. E., Mitrovica, J. X., & Webster, J. M. (2013). Ice sheet collapse following a prolonged period of stable sea level during the last interglacial. *Nature Geoscience*, *6*, 796–800. https://doi.org/10.1038/ngeo1890

Oleson, K. W., Niu, G. Y., Yang, Z. L., Lawrence, D. M., Thornton, P. E., Lawrence, P. J., … Qian, T. (2008). Improvements to the Community Land Model and their impact on the hydrological cycle. *Journal of Geophysics Research*, *113*, G01021. https://doi.org/10.1029/2007JG000563

Otto-Bliesner, B. L., Marsha, S. J., Overpeck, J. T., Miller, G. H., Hu, A. X., & Mem, C. L. I. P. A. (2006). Simulating Arctic climate warmth and icefield retreat in the last interglaciation. *Science*, *311*, 1751–1753. https://doi.org/10.1126/science.1120808

Otto-Bliesner, B. L., Rosenbloom, N., Stone, E. J., McKay, N. P., Lunt, D. J., Brady, E. C., & Overpeck, J. T. (2013). How warm was the last interglacial? New model data comparisons. *Philosophical Transactions of the Royal Society of London, Series A: Mathematical, Physical and Engineering Sciences*, *371*, 20130097. https://doi.org/10.1098/rsta.2013.0097

Payne, A. J. (1999). A thermomechanical model of ice flow in West Antarctica. *Climate Dynamics*, *15*, 115–125. https://doi.org/10.1007/s003820050271

Past Interglacials Working Group of PAGES (2016). Interglacials of the last 800,000 years. *Reviews of Geophysics*, *54*, 162–219. https://doi.org/10.1002/2015RG000482

Quiquet, A., Ritz, C., Punge, H. J., & Salas y Milia, D. (2013). Greenland ice sheet contribution to sea level rise during the last interglacial period: A modelling study driven and constrained by ice core datA. *Climate of the Past*, *9*, 353–366. https://doi.org/10.5194/cp-9-353-2013

Rachmayani, R., Prange, M., & Schulz, M. (2015). North African vegetation-precipitation feedback in early and mid-Holocene climate simulations with CCSM3-DGVM. *Climate of the Past*, *11*, 175–185. https://doi.org/10.5194/cp-11-175-2015

Rachmayani, R., Prange, M., & Schulz, M. (2016). Intra-interglacial climate variability: Model simulations of marine isotope stages 1, 5, 11, 13, and 15. *Climate of the Past*, *12*, 677–695. https://doi.org/10.5194/cp-12-677-2016

Raymo, M. E., & Mitrovica, J. X. (2012). Collapse of polar ice sheets during the stage 11 interglacial. *Nature*, *483*(7390), 453–456. https://doi.org/10.1038/nature10891

Reeh, N. (1991). Paramterization of melt rate and surface temperature on the Greenland ice-sheet. *Polarforschung*, *59*, 113–128.

Reyes, A. V., Carlson, A. E., Beard, B. L., Hatfield, R. G., Stoner, J. S., Winsor, K., … Welke, B. (2014). South Greenland ice-sheet collapse during Marine Isotope Stage 11. *Nature*, *510*, 525–528. https://doi.org/10.1038/nature13456

Roberts, D. L., Karkanas, P., Jacobs, Z., Marean, C. W., & Roberts, R. G. (2012). Melting ice sheets 400,000 yr ago raised sea level by 13 m: Past analogue for future trends. *Earth Planet, Science Letters*, *357*, 226–237. https://doi.org/10.1016/j.epsl.2012.09.006

Robinson, A., Alvarez-Solas, J., Calov, R., Ganopolski, A., & Montoya, M. (2017). MIS-11 duration key to disappearance of the Greenland ice sheet. *Nature Communications*, *8*, 16008. https://doi.org/10.1038/ncomms16008

Robinson, A., Calov, R., & Ganopolski, A. (2011). Greenland ice sheet model parameters constrained using simulations of the Eemian Interglacial. *Climate of the Past*, *7*, 381–396. https://doi.org/10.5194/cp-7-381-2011

Robinson, A., Calov, R., & Ganopolski, A. (2012). Multistability and critical thresholds of the Greenland ice sheet. *Nature Climate Change*, *2*, 429–432. https://doi.org/10.1038/nclimate1449

Rutt, I. C., Hagdorn, M., Hulton, N. R. J., & Payne, A. J. (2009). The Glimmer community ice sheet model. *Journal of Geophysical Research*, *114*, F02004. https://doi.org/10.1029/2008JF001015

Schaefer, J. M., Finkel, R. C., Balco, G., Alley, R. B., Caffee, M. W., Briner, J. P., … Schwartz, R. (2016). Greenland was nearly ice-free for extended periods during the Pleistocene. *Nature*, *540*, 252–255. https://doi.org/10.1038/nature20146

Schilt, A., Baumgartner, M., Blunier, T., Schwander, J., Spahni, R., Fischer, H., & Stocker, T. F. (2010). Glacial-interglacial and millennial-scale variations in the atmospheric nitrous oxide concentration during the last 800,000 years. *Quaternary Science Reviews*, *29*, 182–192.

Stommel, H. (1961). Thermohaline convection with two stable regimes of flow. *Tellus*, *13*, 224–230. https://doi.org/10.1111/j.2153-3490.1961.tb00079.x

Stone, E. J., Lunt, D. J., Annan, J. D., & Hargreaves, J. C. (2013). Quantification of the Greenland ice sheet contribution to last interglacial sea-level-rise. *Climate of the Past*, *9*, 621–639. https://doi.org/10.5194/cp-9-621-2013

Stone, E. J., Lunt, D. J., Rutt, I. C., & Hanna, E. (2010). Investigating the sensitivity of numerical model simulations of the modern state of the Greenland ice-sheet and its future response to climate change. *The Cryosphere*, *4*, 397–417. https://doi.org/10.5194/tc-4-397-2010

Strunk, A., Knudsen, M. F., Egholm, D. L., Jansen, J. D., Levy, L. B., Jacobsen, B. H., & Larsen, N. K. (2017). One million years of glaciation and denudation history in west Greenland. *Nature Communications*, *8*, 14199. https://doi.org/10.1038/ncomms14199

Timmermann, A., & Goosse, H. (2004). Is the wind stress forcing essential for the meridional overturning circulation? *Geophysical Research Letters*, *31*, L04303. https://doi.org/10.1029/2003GL018777

van de Berg, W. J., van den Broeke, M., Ettema, J., van Meijgaard, E., & Kaspar, F. (2011). Significant contribution of insolation to Eemian melting of the Greenland ice sheet. *Nature Geoscience*, *4*, 679–683. https://doi.org/10.1038/ngeo1245

Vazquez Riveiros, N., Waelbroeck, C., Skinner, L., Duplessy, J.-C., McManus, J. F., Kandiano, E. S., & Bauch, H. A. (2013). The "MIS 11 paradox" and ocean circulation: Role of millennial scale events. *Earth and Planetary Science Letters*, *371*, 258–268.

Yang, Q., Dixon, T. H., Myers, P. G., Bonin, J., Chambers, D., & van den Broeke, M. R. (2016). Recent increases in Arctic freshwater flux affects Labrador Sea convection and Atlantic overturning circulation. *Nature Communications*, *7*, 10525. https://doi.org/10.1038/ncomms10525

Yau, A. M., Bender, M. L., Blunier, T., & Jouzel, J. (2016). Setting a chronology for the basal ice at Dye-3 and GRIP: Implications for the long-term stability of the Greenland Ice Sheet. *Earth and Planetary Science Letters*, *451*, 1–9. https://doi.org/10.1016/j.epsl.2016.06.053

Yeager, S. G., Shields, C. A., Large, W. G., & Hack, J. J. (2006). The low-resolution CCSM3. *Journal of Climate*, *19*, 2545–566. https://doi.org/10.1175/JCLI3744.1

Yin, Q. Z., & Berger, A. (2012). Individual contribution of insolation and CO_2 to the interglacial climates of the past 800,000 years. *Climate Dynamics*, *38*, 709–724. https://doi.org/10.1007/s00382-011-1013-5

Yin, Q. Z., & Berger, A. (2015). Interglacial analogues of the Holocene and its natural near future. *Quaternary Science Reviews*, *120*, 28–46. https://doi.org/10.1016/j.quascirev.2015.04.008